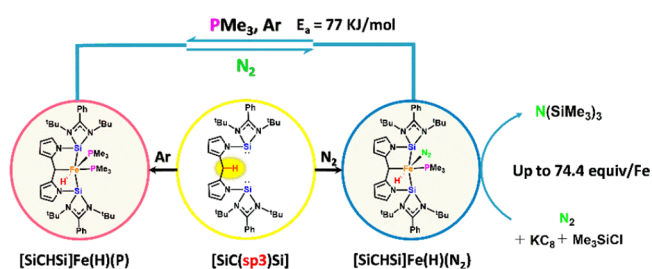


# N<sub>2</sub> Silylation Catalyzed by a Bis(silylene)-Based [SiCsi] Pincer Hydrido Iron(II) Dinitrogen Complex

Shengyong Li, Yajie Wang, Wenjing Yang, Kai Li, Hongjian Sun, Xiaoyan Li,\* Olaf Fuhr, and Dieter Fenske

**ABSTRACT:** The bis(silylene) based SiC(sp<sup>3</sup>)Si pincer ligand *N,N'* bis(LSi)dipyrromethane [SiCH<sub>2</sub>Si] (**L1**; L = PhC(NtBu)<sub>2</sub>) with a C(sp<sup>3</sup>) atom anchor was synthesized, and its coordination chemistry to iron was studied. Two novel iron hydride complexes, [SiCHSi]Fe(H)(N<sub>2</sub>)(PMe<sub>3</sub>) (**1**) and [SiCHSi]Fe(H)(PMe<sub>3</sub>)<sub>2</sub> (**2**), were synthesized in the reaction of **L1** with Fe(PMe<sub>3</sub>)<sub>4</sub> via C(sp<sup>3</sup>)-H bond activation under different inert atmospheres (N<sub>2</sub> and argon). To the best of our knowledge, **1** and **2** are the first examples of a bis(silylene) based hydrido pincer iron complex produced through activation of a C(sp<sup>3</sup>)-H bond. At the same time **1** is also the first example of a TM dinitrogen complex supported by a bis(silylene) ligand. The interconversion between **1** and **2** was achieved and monitored by operando IR and <sup>31</sup>P NMR spectra to understand the transformation from **1** to **2** from the viewpoint of kinetics. To our delight, **1** could effectively catalyze silylation of dinitrogen and gave the highest turnover number so far among all the Fe catalyzed N<sub>2</sub> silylation systems at room temperature and under atmospheric dinitrogen.



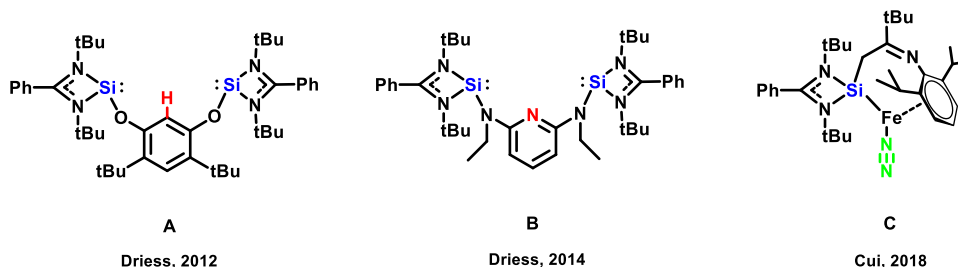
## 1. INTRODUCTION

Suitable ligand frameworks can play a decisive role in steering the reactivity of transition metal (TM) complexes.<sup>1</sup> In recent years, N heterocyclic silylenes (NHSis),<sup>1f,2</sup> heavier analogues of N heterocyclic carbenes (NHCs), have been employed in the activation of small molecules,<sup>3</sup> low valent main group chemistry,<sup>4</sup> and homogeneous catalysis,<sup>1f,5,6</sup> due to the unique  $\sigma$  donating/ $\pi$  accepting and tunable steric hindrance properties. Most notably, the TM complexes stabilized by a variety of silylene ligands have been recognized as superior catalysts in the Suzuki,<sup>7</sup> Heck,<sup>8</sup> Negishi,<sup>9</sup> Kumada,<sup>9-11</sup> and Sonogashira<sup>12</sup> coupling reactions, the regioselective borylation of arenes,<sup>13,14</sup> the cyclotrimerization of alkynes,<sup>15</sup> the hydrosilylation of carbonyl compounds<sup>16-18</sup> or olefins,<sup>19,20</sup> the hydrogenation of olefins<sup>21</sup> or various ketones,<sup>22</sup> and the transfer semi hydrogenation of alkynes to (*E*) olefins.<sup>23</sup> Despite the fact that multidentate donor ligands, especially tridentate pincer like ligands, have the advantages of simultaneously controlling the electronic and spatial properties of TM centers, in comparison to the rich structural diversity of NHC and phosphine ligands, multidentate NHSi ligands remain limited. Up to now, only a few studies involving bis(silylene) pincer ligands have been reported. Driess and co workers reported the synthesis and catalytic application of the bis(silylene)phenyl pincer ligand **A** (termed SiC(sp<sup>2</sup>)Si; Chart 1)<sup>12,13,24</sup> and the bis(silylene)pyridine pincer ligand **B** (termed SiNSi; Chart 1).<sup>14,17,18</sup> A large amount of work has clarified that the sp<sup>3</sup> hybridized carbon coordinated to the metal center highly influences the

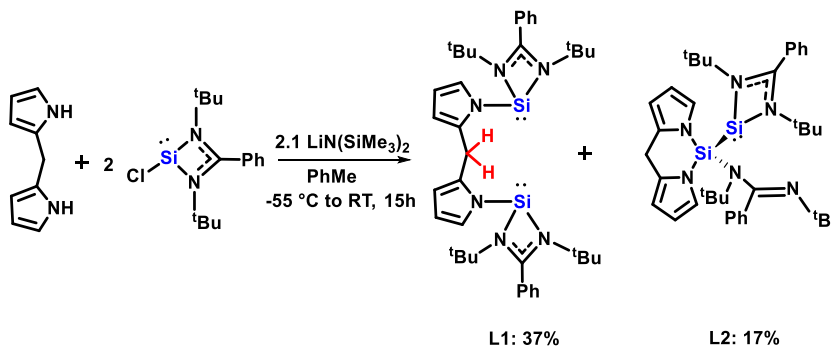
reactivity of the pincer complexes and many significant transformations have been exploited.<sup>25</sup> Our group has been interested in the exploration of the first bis(silylene) based SiC(sp<sup>3</sup>)Si pincer ligand bearing a central sp<sup>3</sup> hybridized carbon as an anchoring site and the construction of an iron based pincer type dinitrogen complex via C(sp<sup>3</sup>)-H activation. To the best of our knowledge, SiC(sp<sup>3</sup>)Si pincer systems involving the activation of the C(sp<sup>3</sup>)-H bond and bis silicon(II) based multidentate ligand supported TM dinitrogen complexes have not been reported so far.

Designing TM dinitrogen complexes for the catalytic N<sub>2</sub> fixation under mild reaction conditions is one of the most important topics in chemistry.<sup>26</sup> In 2003, Schrock and co workers have found the first successful example of the direct and catalytic conversion of dinitrogen into ammonia with a molybdenum catalyst that contains a tetradentate triamidoamine ligand.<sup>27</sup> Since then, extensive studies on the molybdenum catalyzed transformation of N<sub>2</sub> into ammonia and hydrazine under ambient conditions have been reported by some groups.<sup>28</sup> In consideration of the significance of iron at the active sites of nitrogenase enzymes<sup>29</sup> and in the industrial Haber-Bosch process,<sup>30</sup> the preparation of various

Chart 1. Tridentate (Pincer Type) Silylene Ligands A, B and Silylene Iron N<sub>2</sub> Complex C



Scheme 1. Synthesis of the SiC(sp<sup>3</sup>)Si Pincer Type Ligand L1 and Its Isomeride L2



Fe N<sub>2</sub> complexes and the development of iron catalyzed N<sub>2</sub> fixation have attracted increasing attention recently. The Peters, Nishibayashi, and Ashley groups have disclosed catalytic nitrogen fixation systems by using iron dinitrogen complexes bearing P<sub>3</sub>E ligands (E = B, C, Si), anionic PNP type pincer ligands, and diphosphine ligands, respectively.<sup>31–33</sup> It is noteworthy that a very low reaction temperature such as -78 °C is necessary to slow down the direct reaction between the reducing reagents and proton sources in these reaction systems.

As an alternative method of nitrogen fixation, the catalytic reduction of N<sub>2</sub> into tris(trimethylsilyl)amine (N(SiMe<sub>3</sub>)<sub>3</sub>) as an ammonia equivalent has been greatly developed. Since Shiina's precursory work, several TM complexes, including Mo, W, Ti, V, Cr, Fe, and Co, have been found to catalyze the transformation of N<sub>2</sub> into silylamines.<sup>34</sup> As far as the catalytic system containing iron is concerned, in 2012, Nishibayashi found the pioneering example of Fe catalyzed silylation of N<sub>2</sub> under ambient conditions, in which several simple iron complexes such as ferrocenes and Fe(CO)<sub>5</sub> worked as effective catalysts.<sup>35</sup> In 2015, Peters reported the formation of N(SiMe<sub>3</sub>)<sub>3</sub> by using a two coordinated iron complex bearing two cyclic (alkyl)(amine)carbene ligands as a catalyst.<sup>36</sup> After a while, the reductive silylation of N<sub>2</sub> catalyzed by well defined Fe N<sub>2</sub> complexes with a tetradentate P<sub>4</sub>N<sub>2</sub> ligand and a PSiP pincer ligand was disclosed by the Mock and Nishibayashi groups.<sup>37,38</sup> In 2018, Murray and Ashley have reported Fe catalyzed N<sub>2</sub> silylation systems with triiron complexes housed within a tris(β diketiminate)cyclophane and Fe (PP)<sub>2</sub>(N<sub>2</sub>) respectively.<sup>39</sup> More recently, the first silylene supported TM dinitrogen complex, C (Chart 1), which worked as a catalyst to afford up to 47 equiv of silylamine based on the Fe atom of the catalyst, was synthesized by Cui and co workers.<sup>40</sup> Until now, the preparation and reactivity of TM N<sub>2</sub> complexes bearing a bis(silylene) ligand have not been reported.

Herein, we report the facile synthesis and characterization of a novel bis(silylene) based SiC(sp<sup>3</sup>)Si pincer ligand (L1)

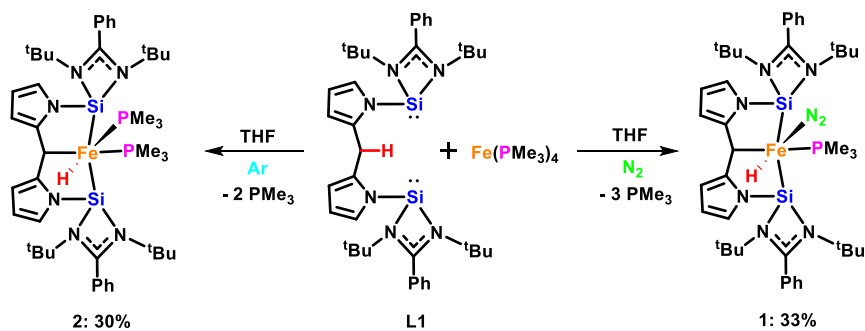
bearing a central sp<sup>3</sup> hybridized carbon as an anchoring site. By the reaction of L1 with Fe(PMe<sub>3</sub>)<sub>4</sub>, two bis(silylene) based hydrido pincer type iron(II) complexes were prepared via C(sp<sup>3</sup>)-H activation. Notably, the hydrido iron(II) dinitrogen complex 1 with a bis(silylene) ligand has been found to work as an effective catalyst for nitrogen fixation with the highest TON so far of all the Fe based N<sub>2</sub> silylation catalysts at room temperature and under atmospheric dinitrogen (up to 74.4 equiv of N(SiMe<sub>3</sub>)<sub>3</sub> per Fe center).<sup>35,36,38,40</sup>

## 2. RESULTS AND DISCUSSION

### 2.1. Synthesis of the SiC(sp<sup>3</sup>)Si Pincer-Type Ligand.

On the basis of our interest in the multidentate NHSi ligands, we intended to synthesize the first bis(silylene) based SiC(sp<sup>3</sup>)Si pincer ligand, featuring a C(sp<sup>3</sup>) atom anchor, through the salt metathesis reactions of bis(pyrrol-2-yl)methane as the backbone (Scheme 1). To a mixture of bis(pyrrol-2-yl)methane and 2 equiv of the chlorosilylene in toluene was dropwise added 2.1 equiv of lithium bis(trimethylsilyl)amide in a toluene solution at -55 °C to afford the desired compound L1. L1 was isolated as colorless lamellar crystals in 37% yield from diethyl ether and fully characterized by <sup>1</sup>H, <sup>13</sup>C, <sup>29</sup>Si NMR spectroscopy and high resolution mass spectrometry (HRMS). The <sup>1</sup>H NMR spectrum of L1 shows two singlets at 1.07 and 5.56 ppm, one for the <sup>t</sup>Bu groups and one corresponding to the CH<sub>2</sub> linkage protons. In the <sup>29</sup>Si NMR spectrum, a singlet resonance signal was detected at -16.4 ppm, which is comparable to that observed for the SiC(sp<sup>2</sup>)Si ligand A and SiNSi ligand B.<sup>17,24</sup> Moreover, the molecular structure of L1 was determined by a preliminary X ray diffraction analysis (see Figure S1 in the Supporting Information). The two N donor stabilized silylene moieties have a similar orientation to form a pre organized pincer "pocket", which is conducive to interaction between the metal center and the C(sp<sup>3</sup>)-H bond. However, the metric parameters are not sufficient for discussion because of the poor crystal quality.

Scheme 2. Synthesis of the SiC(sp<sup>3</sup>)Si Pincer Type Iron Complexes **1** and **2**



To our surprise, in the reaction of dipyrromethane and chlorosilylene, the novel silyl silylene compound **L2** could always be obtained as a byproduct. **L2** was crystallized from *n* pentane in 17% yield. The constitution and structure of **L2** was determined by spectroscopic methods and HRMS. The <sup>29</sup>Si NMR spectrum of **L2** exhibits two singlets at -31.8 and 39.8 ppm for the silyl substituent and low valent silicon center, respectively. In the proposed pathway, the first selective metathesis reaction of deprotonated dipyrromethane with 1 equiv of chlorosilylene was completed. Then intramolecular nucleophilic attack of pyrrole anion toward the Si<sup>II</sup> atom of amidinate stabilized silylene took place and resulted in the cleavage of the Si–N bond in silylene concomitant with the formation of a Si<sup>II</sup>–Si<sup>IV</sup> bond to furnish **L2**. To our knowledge, silyl silylene is scarcely found and usually exists only as a reactive intermediate.<sup>41</sup>

**2.2. Synthesis of [SiCSi]-Pincer Iron(II) Hydrides **1** and **2** via C(sp<sup>3</sup>)–H Activation.** With bis(silylene) based pincer ligand **L1** in hand, we investigated its coordination ability to iron. Surprisingly, the reaction of pincer ligand **L1** with Fe(PMe<sub>3</sub>)<sub>4</sub> in tetrahydrofuran (THF) under an atmospheric pressure of nitrogen gas gave a deep red reaction solution, from which complex **1** was obtained in 33% yield (Scheme 2). In consideration of the reaction of *N,N'* bis(diphenylphosphino) dipyrromethane (PCH<sub>2</sub>P) with Fe(PMe<sub>3</sub>)<sub>4</sub> reported by our group in 2014,<sup>42</sup> N<sub>2</sub> coordination in complex **1** fully illustrates the unique properties of silylene ligands in comparison with diphenylphosphine. Given that nitrogen coordination cannot be achieved in the metalation of the bis silicon(II) based pincer ligands SiC(sp<sup>2</sup>)Si (**A**)<sup>12,13,24</sup> and SiNSi (**B**)<sup>14,17,18</sup> we speculated that a central sp<sup>3</sup> hybridized carbon as an anchoring site has a significant effect on the properties of the complexes and facilitates the coordination of N<sub>2</sub>. To our knowledge, **1** is not only the first example of bis(silylene) based hydrido pincer iron complex produced through activation of the C(sp<sup>3</sup>)–H bond but also the first example of a TM dinitrogen complex supported by a bis(silylene) ligand.

The infrared spectrum of **1** exhibits a strong ν<sub>N≡N</sub> band at 2036 cm<sup>-1</sup> assignable to the terminal dinitrogen ligand and a typical ν<sub>Fe–H</sub> stretching band at 1893 cm<sup>-1</sup>. In comparison with some other iron nitrogen complexes,<sup>31b,38</sup> the slightly lower N–N stretching frequency of **1** suggests that the bis(silylene) based [SiCSi] pincer ligand **L1** has good electron donating ability to enhance back bonding from the iron center to the coordinated dinitrogen ligand. In the <sup>31</sup>P NMR spectrum of **1**, the signal of the PMe<sub>3</sub> ligand appears at 24.8 ppm as a singlet. In the <sup>1</sup>H NMR spectrum of **1**, the characteristic hydrido signal as a doublet peak was found at -16.80 ppm with a J<sub>P–H</sub> coupling constant of 25.2 Hz. The C<sub>s</sub> symmetry of **1** in

solution was revealed by the <sup>29</sup>Si NMR spectrum of **1**, which shows a doublet (J<sub>P–Si</sub> = 38.7 Hz) at 72.3 ppm, highlighting the equivalency of both silicon atoms. The <sup>29</sup>Si NMR spectrum is significantly shifted downfield in comparison to that of **L1**, which is an indication of the reduced electron density on the silicon atom.

Single crystals of **1** suitable for X ray analysis were obtained from Et<sub>2</sub>O at room temperature. **1** has a distorted octahedral geometry around the iron atom (Figure 1). The Fe1–H bond

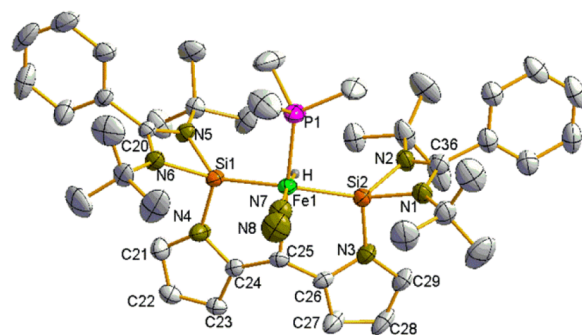


**Figure 1.** Molecular structure of compound **1**. Thermal ellipsoids are drawn at the 50% probability level. Hydrogen atoms except for Fe–H are omitted for clarity. Selected bond lengths (Å) and angles (deg): Fe1–H 1.42(5), Fe1–P1 2.189(1), Fe1–N7 1.798(3), Fe1–Si1 2.172(1), Fe1–Si2 2.171(1), Fe1–C25 2.186(3), N7–N8 1.120(5); P1–Fe1–C25 178.9(1), H–Fe1–N7 171(2), Si1–Fe1–Si2 142.40(4), Si1–Fe1–H 76(2), Si2–Fe1–H 69(2), Si1–Fe1–N7 106.4(1), Si2–Fe1–N7 107.0(1), Si1–Fe1–C25 82.36(9).

length of 1.42(5) Å is similar to that of the disilylene iron hydride [(Si,N)(Si,C)Fe(H)(PMe<sub>3</sub>)].<sup>43</sup> The N7–N8 (1.120(5) Å) and Fe1–N7 (1.798(3) Å) bond lengths lie in the range of those in the known terminal nitrogen Fe complexes (1.101–1.154 and 1.759–1.857 Å, respectively).<sup>32,33,37–40</sup> Both Fe–Si bonds (2.17 Å) are shorter than those in silylene→Fe(CO)<sub>4</sub> complexes (:Si(N<sup>t</sup>BuCH)<sub>2</sub>, 2.196 Å; O<sup>t</sup>Bu(N<sup>t</sup>Bu)<sub>2</sub>CPh, 2.237(7) Å)<sup>44</sup> and comparable to those for Fe=Si bonds reported by Tobita<sup>45</sup> and Driess.<sup>17</sup> This result indicates the formation of significant back bonding from Fe to Si. The above observation fully elucidates that bis(silylene) based pincer ligand **L1** could be considered as not only a particularly strong σ donor but also a π acceptor.

The successful coordination of N<sub>2</sub> in **1** prompted us to explore the construction of the highly electron rich hydrido NHSi iron complexes, which have great potential application in catalytic systems. Treatment of **L1** with Fe(PMe<sub>3</sub>)<sub>4</sub> under an argon atmosphere in THF at room temperature for 24 h gave a deep red reaction solution, from which orange crystals **2** were

isolated upon workup (30% yield) (Scheme 2). The structural details of **2** in the solid state were established by single crystal X ray diffraction analysis (Figure 2). The molecular structure

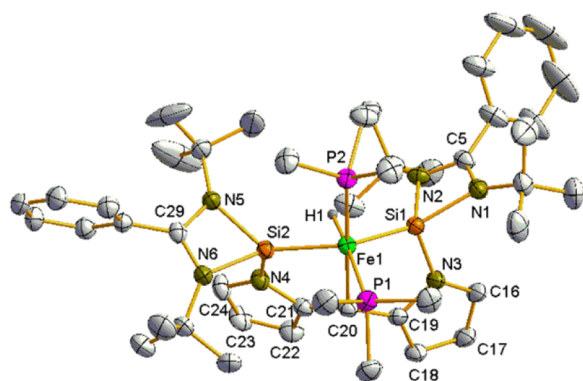


**Figure 2.** Molecular structure of compound **2**. Thermal ellipsoids are drawn at the 50% probability level. Hydrogen atoms except for Fe–H are omitted for clarity. Selected bond lengths (Å) and angles (deg): Fe1–H1 1.37(2), Fe1–P1 2.2097(7), Fe1–P2 2.1738(7), Fe1–Si1 2.1758(7), Fe1–Si2 2.1787(7), Fe1–C20 2.216(2); H1–Fe1–P1 174.7(9), Si1–Fe1–Si2 133.65(3), P2–Fe1–C20 174.59(6), H1–Fe1–Si1 71.5(9), H1–Fe1–Si2 66.3(9), P1–Fe1–Si1 110.10(3), P1–Fe1–Si2 110.42(3), C20–Fe1–Si2 79.85(6).

of **2** shows characteristics similar to those of **1**. Owing to the greater steric congestion around the iron center, **2** has a more distorted hexacoordinate octahedral geometry with [P2Si1C20Si2] as the equatorial plane. The axial Fe1–P1 bond (2.210 Å) features a slightly longer bond distance in comparison to the Fe1–P2 bond (2.174 Å) situated at the equatorial position, presumably due to the strong *trans* influence of the hydrido H ligand. The Fe1–H1 bond of 1.37(2) Å is slightly shorter than that in **1**.

It is noteworthy that the  $^1\text{H}$ ,  $^{13}\text{C}$ ,  $^{31}\text{P}$ , and  $^{29}\text{Si}$  NMR spectra of isolated crystals of complex **2** exhibit two sets of signals related to two flexible isomers (see the Supporting Information for more details). For instance, the  $^1\text{H}$  NMR spectrum of **2** in acetone  $d_6$  exhibits two signals at  $-13.06$  and  $-15.50$  ppm, two resonances at 3.98 and 3.68 ppm, four singlets at 1.03, 1.09, 1.32, and 1.38 ppm with relative ratios of 1:1.3, 1:1.3, and 18:18:(18  $\times$  1.3):(18  $\times$  1.3), respectively. These signals were unambiguously assigned to hydrido, the C(sp $^3$ )–H of the dipyrromethane moiety, and the  $^t\text{Bu}$  group of silylene, respectively. In the  $^{31}\text{P}$  NMR spectrum of **2**, four doublets, at 15.8, 19.7, 20.2, and 23.6 ppm, could be divided into two groups ( $J_{\text{P-P}} = 41.1$  Hz, 23.0 Hz). The fluxional behavior of **2** in solution is also consistent with the information from infrared (IR) spectra. The infrared spectrum of the pure crystals of **2** shows a weak absorption at  $1890\text{ cm}^{-1}$  assignable to Fe–H. However, two weak Fe–H bands appear at 1883 and  $1841\text{ cm}^{-1}$  in a  $\text{C}_6\text{D}_6$  solution. The result also shows that **2** has two isomers in solution.

**2.3. Mutual Transformation between 1 and 2 and Kinetic Study.** Complex **1** appears to be very stable in the solid state as well as in solution under an  $\text{N}_2$  atmosphere. Although complex **2** has a very robust structure in the solid state under an argon atmosphere, it will dissociate the  $\text{PMe}_3$  ligand very slowly in solution. The signal of dissociated  $\text{PMe}_3$  could be detected at  $-61.7$  ppm after **2** was dissolved in  $\text{C}_6\text{D}_6$  for 20 h. The slight instability of **2** in solution can be rationalized by the strong *trans* effect of the hydride ligand and steric hindrance, as indicated by a space filling model of **2** (see Figure S2 in the Supporting Information). Encouraged by these results, we have achieved the interconversion between **1** and **2** by the selection of suitable reaction conditions (Figure 3). Treatment of **1** with  $\text{PMe}_3$  (excess) in THF under an argon atmosphere afforded **2** through the ligand replacement of  $\text{N}_2$  by  $\text{PMe}_3$ . When a solution of **2** was exposed to  $\text{N}_2$  in THF at

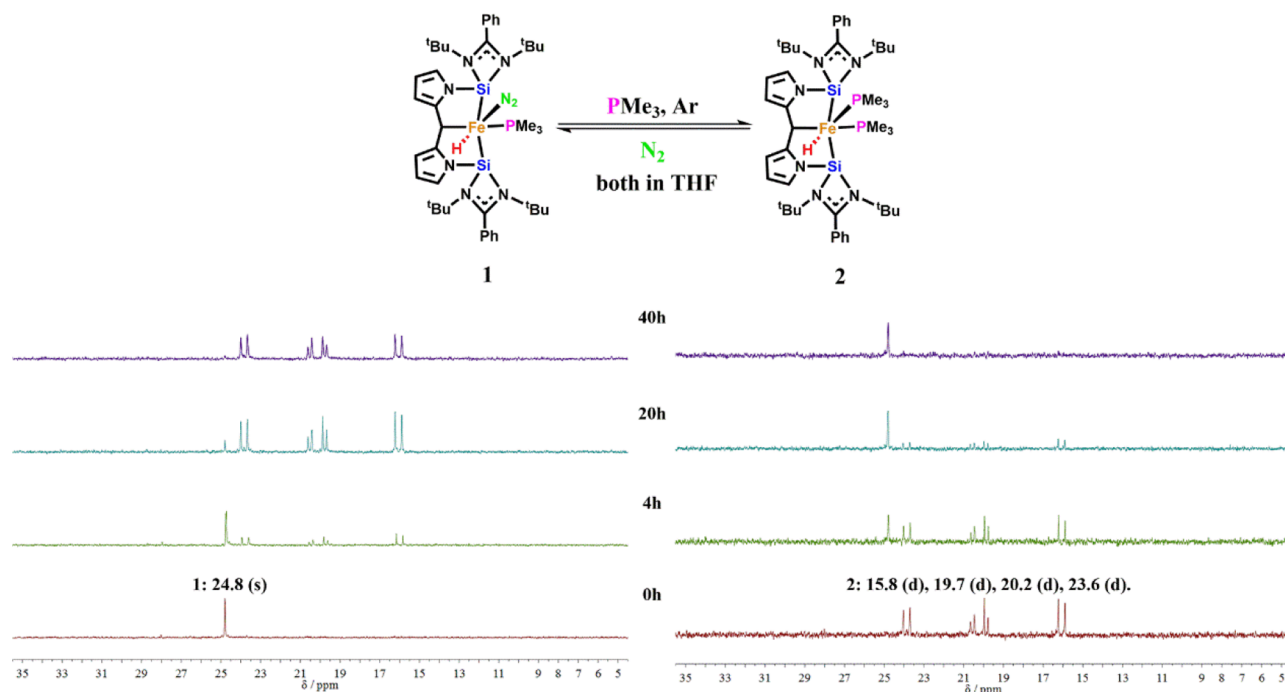


**Figure 3.** (top) Mutual transformation between **1** and **2** under specific conditions. (bottom)  $^{31}\text{P}$  NMR spectra (left, **1** to **2**; right, **2** to **1**) recorded for the corresponding reaction in THF at specific times.

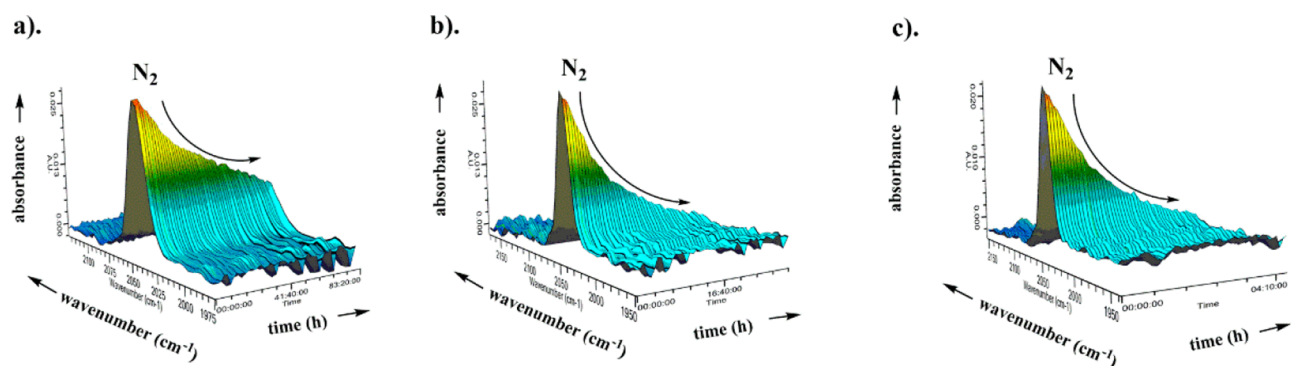


**Figure 4.** 3D kinetic profile of the reaction of complex **1** with 30 equiv of  $\text{PMe}_3$  in 5 mL of THF at various temperatures: (a) 273 K; (b) 293 K; (c) 307 K. The initial concentration of **1** was  $0.02338 \text{ mol L}^{-1}$ .

room temperature, **1** was obtained by ligand exchange. As shown in Figure 3, we recorded the  $^{31}\text{P}$  NMR spectra of both transformations at the given times to monitor the progress. Remarkably, the reactions were fully completed at last, as judged from a  $^{31}\text{P}$  NMR study.

Intrigued by the interesting equilibrium between **1** and **2**, we were curious about how it would affect the rate if the concentration of  $\text{PMe}_3$  were to be changed. In the transformation from **1** to **2**, the kinetic data for different initial concentrations of  $\text{PMe}_3$  at the early stage of the reaction were recorded by the  $^{31}\text{P}$  NMR spectra (see Table S2 and Figure S3 in the Supporting Information). The plot of  $\nu(2)$  against the concentration of  $\text{PMe}_3$  showed that  $\nu(2)$  apparently depended on  $[\text{PMe}_3]$ . According to the plot of the  $\log \nu(2)$  vs  $\log[\text{PMe}_3]$ , the reaction order with respect to the  $\text{PMe}_3$  was estimated to be ca. 1.

In order to gain insight into the transformation of **1** into **2**, the reaction between **1** and  $\text{PMe}_3$  was monitored at various temperatures using operando IR (Figure 4 and the Supporting Information). As can be seen from the kinetic profiles of relative absorbance, when **1** was mixed with 30 equiv of  $\text{PMe}_3$  at 273, 293, 296, 305, and 307 K, the absorbance of the terminal dinitrogen ligand decreased gradually. The plot of the integrated absorbance ( $\ln A$ ) of  $\text{N}_2$  against time suggests a linear relationship, which confirms that it is a pseudo first order reaction (see Figures S4–S8 in the Supporting Information). The values of the rate constant  $k_{\text{obs}}$  and  $t_{1/2}$  at various temperatures are summarized in Table 1. The reaction

**Table 1.** Pseudo First Order Rate Constants and Half Lives of the Reaction at Different Temperatures

entry	temp (K)	$k_{\text{obs}}$ ( $\text{s}^{-1}$ )	$t_{1/2}$ (h)
1	273	$3.7 \times 10^{-6}$	51.7
2	293	$2.1 \times 10^{-5}$	9.3
3	296	$3.4 \times 10^{-5}$	5.7
4	305	$1.3 \times 10^{-4}$	1.5
5	307	$1.7 \times 10^{-4}$	1.1

rate was strongly affected by temperature, and  $t_{1/2}$  increased to 51.7 h from 1.1 h. According to the Arrhenius equation, the activation energy  $E_a$  for the ligand exchange in the reaction of **1** to **2** was determined to be ca. 77 kJ/mol. The comparatively large  $E_a$  value provides evidence for strong coordination of the  $\text{N}_2$  ligand in **1**. This is consistent with the remarkable stability, no matter whether in the solid state or in solution. Given that the  $\text{N}_2$  binding affinity is a very important parameter that can

influence catalytic activity toward nitrogen fixation,<sup>36,37</sup> we further believe that SiCSi pincer iron dinitrogen complex **1** could be an effective catalyst toward the silylation of  $\text{N}_2$ .

#### 2.4. Catalytic Nitrogen Fixation Using **1** as Catalyst.

The investigation of catalytic silylation of dinitrogen gas was carried out by using complex **1** as a catalyst under ambient reaction conditions. The results are summarized in Table 2.

**Table 2.** Catalytic Silylation of Molecular Dinitrogen Using Complex **1**<sup>a</sup>

$$\text{N}_2 + n \text{ Reductant} + n \text{ Me}_3\text{SiCl} \xrightarrow[\text{Solvent}]{\text{1 (0.01 mmol)}} 2 \text{ N(SiMe}_3)_3$$

entry	reductant (M)	solvent	$T$ ( $^{\circ}\text{C}$ )	reductant/ $\text{ClSiMe}_3$ (equiv) <sup>b</sup>	$\text{N(SiMe}_3)_3$ (equiv) <sup>b,c</sup>
1	Li	THF	25	600	trace
2	Na	THF	25	600	1.3
3	K	THF	25	600	2.9
4	$\text{KC}_8$	THF	25	600	10.5
5	$\text{KC}_8$	<i>n</i> -pentane	25	600	4.7
6	$\text{KC}_8$	toluene	25	600	5.3
7	$\text{KC}_8$	$\text{Et}_2\text{O}$	25	600	6.5
8	$\text{KC}_8$	DME	25	600	6.6
9	$\text{KC}_8$	dioxane	25	600	20.8
10	$\text{KC}_8$	dioxane	50	600	19.9
11	$\text{KC}_8$	dioxane	80	600	19.7
12 <sup>d</sup>	$\text{KC}_8$	dioxane	25	600	trace
13 <sup>e</sup>	$\text{KC}_8$	dioxane	25	600	13.4
14 <sup>f</sup>	$\text{KC}_8$	dioxane	25	600	trace
15	$\text{KC}_8$	dioxane	25	1800	40.3
16 <sup>g</sup>	$\text{KC}_8$	dioxane	25	1800	74.4

<sup>a</sup>Experiments performed over 20 h in 20 mL of solvent using 0.01 mmol of the catalyst under  $\text{N}_2$ , unless otherwise stated. Yields are an average. <sup>b</sup>Based on the catalyst. <sup>c</sup>Determined by GC. <sup>d</sup>Using 0.01 mmol of free ligand **1**. <sup>e</sup>Using 0.01 mmol of **2** instead of **1**. <sup>f</sup>Using 0.01 mmol of  $[\text{PCHP}]\text{Fe}(\text{H})(\text{PMe}_3)^{41}$  instead of **1**. <sup>g</sup>Conducted for 150 h.

The reaction of  $\text{N}_2$  (1 atm) with  $\text{KC}_8$  (600 equiv based on **1**) as a strong reductant and  $\text{Me}_3\text{SiCl}$  (600 equiv based on **1**) as the silylating reagent in the presence of **1** as catalyst in THF at room temperature for 20 h gave 10.5 equiv of  $\text{N(SiMe}_3)_3$  based on the iron atom (Table 2, entry 4). The  $\text{N(SiMe}_3)_3$  was confirmed as a product by gas chromatography (GC) and HRMS. Using various alkali metals (Li, Na, K) in place of  $\text{KC}_8$ , a lower amount of  $\text{N(SiMe}_3)_3$  was produced because of the

weaker reducing ability or smaller specific surface area (Table 2, entries 1–3). It is worth noting that the solvent polarity has a great influence on the yields (Table 2, entries 4–9). The reaction in dioxane afforded the highest yield (20.8 equiv). In comparison with the reaction in *n* pentane, the yield was increased by 4 times. Interestingly, the reaction temperature has little influence on the yield (Table 2, entries 9–11). The control experiments indicate that complex **1** is necessary for the catalytic formation of  $\text{N}(\text{SiMe}_3)_3$  (Table 2, entries 12). A 13.4 equiv amount of  $\text{N}(\text{SiMe}_3)_3$  was produced when complex **2** was used as the catalyst (Table 2, entry 13). The poor catalytic behavior of  $[\text{PCHP}]\text{Fe}(\text{H})(\text{PMe}_3)^{42}$  fully illustrated the significant role of the bis(silylene)dipyrromethane ligand (Table 2, entry 14). With a larger amount of  $\text{KC}_8$  and  $\text{Me}_3\text{SiCl}$ , the catalytic reactions gave 40.3 equiv (a 7% yield, based on  $\text{KC}_8$ ) in 20 h and 74.4 equiv (a 13% yield, based on  $\text{KC}_8$ ) of  $\text{N}(\text{SiMe}_3)_3$  in 150 h per Fe atom. This represents a very high TON in comparison to the Fe based  $\text{N}_2$  silylation catalysts reported to date (Table 2, entries 15 and 16).<sup>35–38,40</sup> We monitored the time profile of the catalytic reactions using **1** as the catalyst (see the Supporting Information for the detailed procedure). The result is shown in Figure 5. The catalytic formation of  $\text{N}(\text{SiMe}_3)_3$  proceeded rapidly and was almost complete after 150 h.

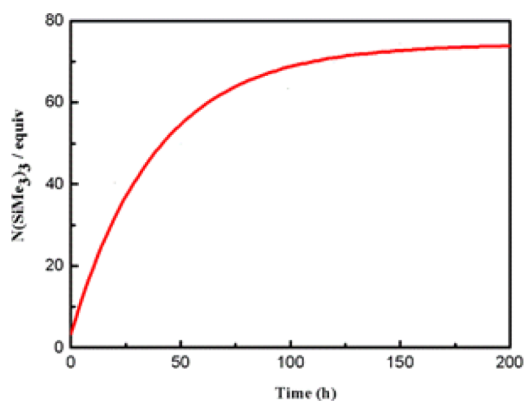


**Figure 5.** Time profile of the formation of  $\text{N}(\text{SiMe}_3)_3$  using **1** as catalyst.

A filtration test, whereby insoluble and soluble specimens were separated by filtration and independently assayed for catalytic activity, was conducted to exclude the possibility that Fe nanoparticles work as true active species in the present reaction system (see the Supporting Information for the detailed procedure).

Encouraged by these experimental results, we were interested in the investigation of the catalytic behavior from the viewpoint of a kinetic study (see the Supporting Information for more details). The kinetic data for different initial concentrations of catalyst **1** at the early stage of the reaction were calculated (Table S4 and Figure S10). The plot of  $\nu(\text{N}(\text{SiMe}_3)_3)$  against the concentration of Fe showed that  $\nu(\text{N}(\text{SiMe}_3)_3)$  apparently depended on  $[\text{Fe}]$  when complex **1** was used as a catalyst. According to a plot of  $\log \nu(\text{N}(\text{SiMe}_3)_3)$  vs  $\log [\text{Fe}]$ , the reaction order with respect to the Fe was estimated to be ca. 1. Unfortunately, no reactive intermediates have yet been isolated from the stoichiometric reaction of **1** with  $\text{KC}_8$  and  $\text{Me}_3\text{SiCl}$ .

Although Murray and Ashley have reported Fe catalyzed  $\text{N}_2$  silylation systems with higher yields (83 and 121 equiv,

respectively),<sup>39</sup> a very low reaction temperature or an elevated pressure must be used to increase yields. In all of the Fe catalyzed  $\text{N}_2$  silylation systems at room temperature and with atmospheric dinitrogen, complex **1** gave the highest turnover number to date.

### 3. CONCLUSIONS

In summary, the novel bis(silylene) based  $\text{SiC}(\text{sp}^3)\text{Si}$  pincer ligand **L1** bearing a central  $\text{sp}^3$  hybridized carbon as an anchoring site was synthesized by a salt metathesis reaction of chlorosilylene with deprotonated dipyrromethane. Meanwhile, the rare silyl silylene complex **L2** was obtained as a byproduct. By the reactions of **L1** with  $\text{Fe}(\text{PMe}_3)_4$  under different inert atmospheres ( $\text{N}_2$  and argon), two novel iron hydride complexes,  $[\text{SiCHSi}]\text{Fe}(\text{H})(\text{N}_2)(\text{PMe}_3)$  (**1**) and  $[\text{SiCHSi}]\text{Fe}(\text{H})(\text{PMe}_3)_2$  (**2**), were synthesized via  $\text{C}(\text{sp}^3)\text{--H}$  bond activation. To our knowledge, **1** and **2** are the first examples of bis(silylene) based hydrido pincer iron complexes produced through activation of the  $\text{C}(\text{sp}^3)\text{--H}$  bond; at the same time, **1** is also the first example of a TM dinitrogen complex supported by a bis(silylene) ligand. Mutual transformations between complexes **1** and **2** in solution were achieved by the selection of suitable reaction conditions. Operando IR was used to monitor the whole reaction process to gain insight into the transformation of **1** into **2**. The activation energy  $E_a$  for the ligand exchange in the reaction of **1** to **2** was determined to be 77 kJ/mol, which is comparatively large, providing an evidence for robust coordination of the  $\text{N}_2$  ligand in **1**. Remarkably, the hydrido iron nitrogen complex **1** with a bis(silylene) ligand could be an effective catalyst for nitrogen fixation. **1** presents the highest turnover number to date of all the Fe catalyzed  $\text{N}_2$  silylation systems at room temperature and under atmospheric dinitrogen (1 atm). Kinetic studies demonstrated that the reaction order with respect to the Fe was estimated to be ca. 1. We believe that our work will provide some new strategies and strongly promote the further development of N heterocyclic silylene chemistry and nitrogen fixation under mild conditions catalyzed by transition metal dinitrogen complexes. Detailed mechanistic studies and further modifications of the ligand are currently being explored in our laboratory.

### 4. EXPERIMENTAL SECTION

**4.1. General Considerations.** Infrared spectra ( $4000\text{--}400\text{ cm}^{-1}$ ) were recorded on a Bruker ALPHA FT IR instrument by using Nujol mulls between KBr disks. The  $^1\text{H}$ ,  $^{13}\text{C}$ ,  $^{31}\text{P}$ , and  $^{29}\text{Si}$  NMR spectra were recorded with a Bruker 300 spectrometer. High resolution mass spectra (HRMS) were obtained using an electrospray ionization time of flight (ESI TOF) mass spectrometer. Melting points (mp) were measured on a WRR instrument with samples sealed in capillaries. Gas chromatography (GC) was performed with *n* dodecane as an internal standard. All experiments and manipulations were carried out under a nitrogen atmosphere using standard Schlenk techniques, unless otherwise noted. All solvents were dried by general methods and freshly distilled before use. Chlorosilylene,<sup>46</sup>  $\text{Fe}(\text{PMe}_3)_4$ <sup>47</sup> and  $\text{KC}_8$ <sup>48</sup> were prepared according to the reported procedures.

**4.2. Synthesis of Pincer-Type Ligand **L1** and Silyl-Silylene **L2**.** To a solution of dipyrromethane (1.68 g, 11.3 mmol) and chlorosilylene (6.68 g, 22.7 mmol) in toluene (80 mL) was added a solution of  $\text{LiN}(\text{SiMe}_3)_2$  (3.98 g, 23.8 mmol) in toluene (70 mL) at  $-55\text{ }^\circ\text{C}$  under  $\text{N}_2$ . After the mixture was stirred for 1 h, the resulting solution was warmed to room temperature and stirred overnight. The solvents were removed under vacuum, and the residue was extracted with *n* pentane and  $\text{Et}_2\text{O}$ . The organic solutions were concentrated slowly in vacuo and further cooled in the freezer at  $-20\text{ }^\circ\text{C}$ .

**L1** was obtained as colorless lamellar crystals from diethyl ether (2.76 g, 37%). Mp: 69–70 °C. <sup>1</sup>H NMR (300 MHz, C<sub>6</sub>D<sub>6</sub>, 298 K): δ (ppm) 1.07 (s, 36H, NC(CH<sub>3</sub>)<sub>3</sub>), 5.56 (s, 2H, –CH<sub>2</sub>–), 6.62 (d, *J* = 18.0 Hz, 4H, arom, C–H), 6.90–6.96 (m, 8H, arom, C–H), 7.05–7.07 (m, 2H, arom, C–H), 7.13 (br s, 2H, arom, C–H). <sup>13</sup>C NMR (75 MHz, C<sub>6</sub>D<sub>6</sub>, 298 K): δ (ppm) 15.3 (–CH<sub>2</sub>–), 31.3 (NC(CH<sub>3</sub>)<sub>3</sub>), 53.0 (NC(CH<sub>3</sub>)<sub>3</sub>), 109.4 (C<sub>arom</sub>), 110.1 (C<sub>arom</sub>), 119.9 (C<sub>arom</sub>), 127.5 (C<sub>arom</sub>), 129.3 (C<sub>arom</sub>), 129.9 (C<sub>arom</sub>), 133.9 (C<sub>arom</sub>), 139.5 (C<sub>arom</sub>), 163.9 (NCN). <sup>29</sup>Si NMR (59.59 MHz, C<sub>6</sub>D<sub>6</sub>, 298 K): δ (ppm) –16.4 (s). HRMS (ESI TOF): 663.4026 [M + H]<sup>+</sup>; calcd for C<sub>39</sub>H<sub>55</sub>N<sub>6</sub>Si<sub>2</sub>, 663.4027. Anal. Calcd for C<sub>39</sub>H<sub>54</sub>N<sub>6</sub>Si<sub>2</sub>: C, 70.65; H, 8.21; N, 12.67. Found: C, 70.29; H, 8.10; N, 12.48.

**L2** was crystallized from *n* pentane as a green virgulate crystal (1.26 g, 17%). Dec pt: >133 °C. <sup>1</sup>H NMR (300 MHz, C<sub>6</sub>D<sub>6</sub>, 298 K): δ (ppm) 1.08 (s, 18H, NC(CH<sub>3</sub>)<sub>3</sub>), 1.22 (s, 9H, NC(CH<sub>3</sub>)<sub>3</sub>), 1.43 (s, 9H, NC(CH<sub>3</sub>)<sub>3</sub>), 4.41 (dd, *J* = 33.9, 17.4 Hz, 2H, –CH<sub>2</sub>–), 6.31 (br s, 2H, arom, C–H), 6.50 (t, *J* = 3.0 Hz, 2H, arom, C–H), 6.85–6.88 (m, 1H, arom, C–H), 6.94–7.03 (m, 4H, arom, C–H), 7.08–7.15 (m, 3H, arom, C–H), 7.48–7.50 (m, 2H, arom, C–H), 7.66 (br s, 2H, arom, C–H). <sup>13</sup>C NMR (75 MHz, C<sub>6</sub>D<sub>6</sub>, 298 K): δ (ppm) 27.1 (–CH<sub>2</sub>–), 31.1 (NC(CH<sub>3</sub>)<sub>3</sub>), 53.6 (NC(CH<sub>3</sub>)<sub>3</sub>), 107.1 (C<sub>arom</sub>), 109.9 (C<sub>arom</sub>), 124.5 (C<sub>arom</sub>), 127.2 (C<sub>arom</sub>), 127.4 (C<sub>arom</sub>), 128.3 (C<sub>arom</sub>), 129.2 (C<sub>arom</sub>), 129.4 (C<sub>arom</sub>), 131.0 (C<sub>arom</sub>), 132.9 (C<sub>arom</sub>), 134.5 (C<sub>arom</sub>), 141.9 (C<sub>arom</sub>), 157.7 (N–C = N), 161.7 (NCN). <sup>29</sup>Si NMR (59.59 MHz, C<sub>6</sub>D<sub>6</sub>, 298 K): δ (ppm) 39.8 (s, Si), –31.8 (s, Si). HRMS (ESI TOF): 663.4037 [M + H]<sup>+</sup>; calcd for C<sub>39</sub>H<sub>55</sub>N<sub>6</sub>Si<sub>2</sub>, 663.4021. Anal. Calcd for C<sub>39</sub>H<sub>54</sub>N<sub>6</sub>Si<sub>2</sub>: C, 70.65; H, 8.21; N, 12.67. Found: C, 70.32; H, 8.12; N, 12.50.

#### 4.3. Synthesis of SiCSi Pincer-Type Iron Dinitrogen Complex 1.

A solution of ligand **L1** (2.17 g, 3.3 mmol) in THF (75 mL) was added slowly to a solution of Fe(PMe<sub>3</sub>)<sub>4</sub> (1.41 g, 3.9 mmol) in THF (75 mL) at –78 °C under N<sub>2</sub>. The reaction mixture was warmed to room temperature and stirred for 24 h, resulting in a dark red solution. The volatiles were removed in vacuo, and the residue was extracted with pentane and diethyl ether. Complex **1** (0.89 g) was isolated as orange block crystals in 33% yield at room temperature. Dec pt: >184 °C. IR (Nujol mull, KBr, cm<sup>–1</sup>): 2036 ν(N≡N), 1893 ν(Fe–H), 942 ρ(PMe<sub>3</sub>). <sup>1</sup>H NMR (300 MHz, C<sub>6</sub>D<sub>6</sub>, 298 K): δ (ppm) –16.80 (d, *J* = 25.2 Hz, 1H, Fe–H), 1.09 (s, 18H, NC(CH<sub>3</sub>)<sub>3</sub>), 1.21 (s, 18H, NC(CH<sub>3</sub>)<sub>3</sub>), 1.61 (d, *J* = 6.6 Hz, 9H, PMe<sub>3</sub>), 4.14 (s, 1H, –FeCH–), 6.86–7.00 (m, 13H, arom, C–H), 7.20–7.26 (m, 3H, arom, C–H). <sup>31</sup>P{<sup>1</sup>H} NMR (121 MHz, C<sub>6</sub>D<sub>6</sub>, 298 K): δ (ppm) 24.8 (s, PMe<sub>3</sub>). <sup>13</sup>C NMR (75 MHz, C<sub>6</sub>D<sub>6</sub>, 298 K): δ (ppm) 25.6 (d, *J* = 18.8 Hz, PMe<sub>3</sub>), 29.9 (FeCH–), 31.3 (NC(CH<sub>3</sub>)<sub>3</sub>), 31.5 (NC(CH<sub>3</sub>)<sub>3</sub>), 53.5 (NC(CH<sub>3</sub>)<sub>3</sub>), 54.3 (NC(CH<sub>3</sub>)<sub>3</sub>), 105.6 (C<sub>arom</sub>), 113.2 (C<sub>arom</sub>), 114.4 (C<sub>arom</sub>), 126.9 (C<sub>arom</sub>), 129.5 (C<sub>arom</sub>), 129.7 (C<sub>arom</sub>), 132.4 (C<sub>arom</sub>), 157.0 (C<sub>arom</sub>), 171.4 (NCN). <sup>29</sup>Si NMR (59.59 MHz, THF (D<sub>2</sub>O), 298 K): δ (ppm) 72.3 (d, *J* = 38.7 Hz). HRMS (ESI TOF): 823.3906 [M + H]<sup>+</sup>; calcd for C<sub>42</sub>H<sub>64</sub>FeN<sub>8</sub>PSi<sub>2</sub>, 823.3880. Anal. Calcd for C<sub>42</sub>H<sub>63</sub>FeN<sub>8</sub>PSi<sub>2</sub>: C, 61.29; H, 7.72; N, 13.62. Found: C, 61.51; H, 7.86; N, 13.51.

#### 4.4. Synthesis of Electron-Rich NHSi Iron Hydride Complex 2.

The synthesis of **2** proceeded in a fashion similar to that for the synthesis of **1** except under an argon atmosphere, with **L1** (1.82 g, 2.8 mmol) and Fe(PMe<sub>3</sub>)<sub>4</sub> (1.19 g, 3.3 mmol). Complex **2** (0.72 g) was isolated as orange red block crystals in 30% yield at room temperature. Dec pt: >167 °C. IR: in solid (Nujol mull, KBr, cm<sup>–1</sup>), 1890 ν(Fe–H); in solution (C<sub>6</sub>D<sub>6</sub>), 1883 and 1841 ν(Fe–H). <sup>1</sup>H NMR (300 MHz, acetone *d*<sub>6</sub>, 298 K): one conformer, δ (ppm) –13.06 (d, *J* = 49.5 Hz, 1H, Fe–H), 0.82 (d, *J* = 3.6 Hz, 9H, PMe<sub>3</sub>), 1.03 (s, 18H, NC(CH<sub>3</sub>)<sub>3</sub>), 1.09 (s, 18H, NC(CH<sub>3</sub>)<sub>3</sub>), 1.50 (d, *J* = 4.2 Hz, 9H, PMe<sub>3</sub>), 3.98 (s, 1H, –FeCH–); another conformer, δ (ppm) –15.50 (dd, *J* = 27.6, 2.4 Hz, 1.3 × 1H, Fe–H), 1.32 (s, 1.3 × 18H, NC(CH<sub>3</sub>)<sub>3</sub>), 1.34 (overlap, 1.3 × 9H, PMe<sub>3</sub>), 1.38 (s, 1.3 × 18H, NC(CH<sub>3</sub>)<sub>3</sub>), 1.64 (d, *J* = 5.4 Hz, 1.3 × 9H, PMe<sub>3</sub>), 3.68 (d, *J* = 12.3 Hz, 1.3 × 1H, –FeCH–); aromatic area (16 + 1.3 × 16), 5.79 (br s, 2H), 6.08 (br s, 6H), 6.60 (d, *J* = 16.8 Hz, 4H), 7.22–7.32 (m, 2H), 7.51–7.61 (m, 18H), 7.80–7.87 (m, 5H). <sup>31</sup>P{<sup>1</sup>H} NMR (121 MHz, acetone *d*<sub>6</sub>, 298 K): one conformer, δ (ppm) 19.7 (d, *J* = 23.0 Hz, 1P, PMe<sub>3</sub>), 20.2 (d, *J* = 23.0 Hz, 1P, PMe<sub>3</sub>); another conformer, δ (ppm)

15.8 (d, *J* = 41.1 Hz, 1.3 × 1P, PMe<sub>3</sub>), 23.6 (d, *J* = 41.1 Hz, 1.3 × 1P, PMe<sub>3</sub>). <sup>13</sup>C NMR (75 MHz, acetone *d*<sub>6</sub>, 298 K): one conformer: δ (ppm) 12.9 (d, *J* = 15 Hz, PMe<sub>3</sub>), 17.4 (d, *J* = 15 Hz, PMe<sub>3</sub>), 30.4 (–FeCH–), 31.2 (NC(CH<sub>3</sub>)<sub>3</sub>), 31.5 (NC(CH<sub>3</sub>)<sub>3</sub>), 53.5 (NC(CH<sub>3</sub>)<sub>3</sub>), 53.9 (NC(CH<sub>3</sub>)<sub>3</sub>), 102.5 (C<sub>arom</sub>), 111.3 (C<sub>arom</sub>), 111.7 (C<sub>arom</sub>), 127.2 (C<sub>arom</sub>), 127.9 (C<sub>arom</sub>), 128.1 (C<sub>arom</sub>), 129.6 (C<sub>arom</sub>), 130.2 (C<sub>arom</sub>), 133.1 (C<sub>arom</sub>), 155.4 (C<sub>arom</sub>), 172.0 (NCN); another conformer, δ (ppm) 24.8 (d, *J* = 15 Hz, PMe<sub>3</sub>), 26.2 (d, *J* = 15 Hz, PMe<sub>3</sub>), 30.6 (FeCH–), 31.9 (NC(CH<sub>3</sub>)<sub>3</sub>), 32.5 (NC(CH<sub>3</sub>)<sub>3</sub>), 54.1 (NC(CH<sub>3</sub>)<sub>3</sub>), 54.3 (NC(CH<sub>3</sub>)<sub>3</sub>), 103.3 (C<sub>arom</sub>), 111.6 (C<sub>arom</sub>), 112.1 (C<sub>arom</sub>), 127.6 (C<sub>arom</sub>), 127.8 (C<sub>arom</sub>), 128.2 (C<sub>arom</sub>), 130.0 (C<sub>arom</sub>), 130.9 (C<sub>arom</sub>), 133.3 (C<sub>arom</sub>), 156.1 (C<sub>arom</sub>), 172.1 (NCN). <sup>29</sup>Si NMR (59.59 MHz, acetone *d*<sub>6</sub>, 298 K): one conformer, δ (ppm) 63.4 (dd, *J* = 40.5, 20.3 Hz); another conformer, δ (ppm) 79.2 (dd, *J* = 41.1, 32.8 Hz). HRMS (ESI TOF): 871.4230 [M + H]<sup>+</sup>; calcd for C<sub>45</sub>H<sub>73</sub>FeN<sub>6</sub>P<sub>2</sub>Si<sub>2</sub>, 871.4260. Anal. Calcd for C<sub>45</sub>H<sub>72</sub>FeN<sub>6</sub>P<sub>2</sub>Si<sub>2</sub>: C, 62.05; H, 8.33; N, 9.65. Found: C, 62.27; H, 8.40; N, 9.75.

**4.5. X-ray Crystal Structure Determinations.** A Bruker Apex II single crystal diffractometer employed Mo Kα radiation (*λ* = 0.71073 Å) or Ga Kα radiation (*λ* = 1.34143) and a CCD area detector. The structure was solved using the charge flipping algorithm, as implemented in the program SUPERFLIP,<sup>49</sup> and refined by full matrix least squares techniques against F<sup>2</sup> (SHELXL)<sup>50</sup> through the OLEX interface.<sup>51</sup> All non hydrogen atoms were refined anisotropically, and all hydrogen atoms except for those of the disordered solvent molecules were placed using AFIX instructions. Appropriate restraints or constraints were applied to the geometry and the atomic displacement parameters of the atoms. CCDC 1846424 (1) and 1876056 (2) contain supplementary crystallographic data for this paper. Copies of the data can be obtained free of charge on application to the CCDC, 12 Union Road, Cambridge CB2 1EZ, U.K. (fax, (+44)1223 336 033; e mail, deposit@ccdc.cam.ac.uk).

## ■ AUTHOR INFORMATION

### Corresponding Author

Xiaoyan Li – School of Chemistry and Chemical Engineering, Key Laboratory of Special Functional Aggregated Materials, Ministry of Education, Shandong University, Jinan 250100, People's Republic of China; [orcid.org/0000 0003 0997 0380](https://orcid.org/0000-0003-0997-0380); Email: xli63@sdu.edu.cn

### Authors

Shengyong Li – School of Chemistry and Chemical Engineering, Key Laboratory of Special Functional Aggregated Materials, Ministry of Education, Shandong University, Jinan 250100, People's Republic of China

Yajie Wang – School of Chemistry and Chemical Engineering, Key Laboratory of Special Functional Aggregated Materials, Ministry of Education, Shandong University, Jinan 250100, People's Republic of China

**Wenjing Yang** – School of Chemistry and Chemical Engineering, Key Laboratory of Special Functional Aggregated Materials, Ministry of Education, Shandong University, Jinan 250100, People's Republic of China

**Kai Li** – School of Chemistry and Chemical Engineering, Key Laboratory of Special Functional Aggregated Materials, Ministry of Education, Shandong University, Jinan 250100, People's Republic of China

**Hongjian Sun** – School of Chemistry and Chemical Engineering, Key Laboratory of Special Functional Aggregated Materials, Ministry of Education, Shandong University, Jinan 250100, People's Republic of China; [orcid.org/0000-0003-1237-3771](https://orcid.org/0000-0003-1237-3771)

**Olaf Fuhr** – Institut für Nanotechnologie (INT) und Karlsruher Nano Micro Facility (KNMF), Karlsruher Institut für Technologie (KIT), 76344 Eggenstein Leopoldshafen, Germany

**Dieter Fenske** – Institut für Nanotechnologie (INT) und Karlsruher Nano Micro Facility (KNMF), Karlsruher Institut für Technologie (KIT), 76344 Eggenstein Leopoldshafen, Germany

## Notes

The authors declare no competing financial interest.

## ACKNOWLEDGMENTS

This work was supported by NSF China 21971151/21572119 and NSF Shandong ZR2019ZD46.

## REFERENCES

- (1) (a) Selander, N.; Szabó, K. J. Catalysis by Palladium Pincer Complexes. *Chem. Rev.* **2011**, *111*, 2048–2076. (b) Asay, M.; Jones, C.; Driess, M. N Heterocyclic Carbene Analogues with Low Valent Group 13 and Group 14 Elements: Syntheses, Structures, and Reactivities of a New Generation of Multitalented Ligands. *Chem. Rev.* **2011**, *111*, 354–396. (c) Sen, S. S.; Khan, S.; Samuel, P. P.; Roesky, H. W. Chemistry of Functionalized Silylenes. *Chem. Sci.* **2012**, *3*, 659–682. (d) Álvarez Rodríguez, L.; Cabeza, J. A.; García Álvarez, P.; Polo, D. The Transition Metal Chemistry of Amidinatosilylenes, germylenes and stannylenes. *Coord. Chem. Rev.* **2015**, *300*, 1–28. (e) Lundgren, R. J.; Stradiotto, M. *Ligand Design in Metal Chemistry: Reactivity and Catalysis*; Wiley: Hoboken, NJ, 2016; pp 1–14. (f) Raoufoghaddam, S.; Zhou, Y. P.; Wang, Y.; Driess, M. N Heterocyclic Silylenes as Powerful Steering Ligands in Catalysis. *J. Organomet. Chem.* **2017**, *829*, 2–10.
- (2) (a) Denk, M.; Lennon, R.; Hayashi, R.; West, R.; Belyakov, A. V.; Verne, H. P.; Haaland, A.; Wagner, M.; Metzler, N. Synthesis and Structure of a Stable Silylene. *J. Am. Chem. Soc.* **1994**, *116*, 2691–2692. (b) Azhakar, R.; Ghadwal, R. S.; Roesky, H. W.; Wolf, H.; Stalke, D. Facile Access to the Functionalized N Donor Stabilized Silylenes PhC(N<sup>t</sup>Bu)<sub>2</sub>SiX (X = PPh<sub>2</sub>, NPh<sub>2</sub>, Ncy<sub>2</sub>, N<sup>t</sup>Pr<sub>2</sub>, NMe<sub>2</sub>, N(SiMe<sub>3</sub>)<sub>2</sub>, O<sup>t</sup>Bu). *Organometallics* **2012**, *31*, 4588–4592. (c) Benedek, Z.; Szilvási, T. Can Low Valent Silicon Compounds Be Better Transition Metal Ligands than Phosphines and NHCs? *RSC Adv.* **2015**, *5*, 5077–5086.
- (3) (a) Azhakar, R.; Roesky, H. W.; Wolf, H.; Stalke, D. On the Reactivity of the Silylene PhC(N<sup>t</sup>Bu)<sub>2</sub>SiNPh<sub>2</sub> toward Organic Substrates. *Z. Anorg. Allg. Chem.* **2013**, *639*, 934–938. (b) Mo, Z.; Szilvási, T.; Zhou, Y. P.; Yao, S.; Driess, M. An Intramolecular Silylene Borane Capable of Facile Activation of Small Molecules, Including Metal Free Dehydrogenation of Water. *Angew. Chem., Int. Ed.* **2017**, *56*, 3699–3702. (c) Wang, Y.; Kostenko, A.; Hadlington, T. J.; Luecke, M. P.; Yao, S.; Driess, M. Silicon Mediated Selective

Homo and Heterocoupling of Carbon Monoxide. *J. Am. Chem. Soc.* **2019**, *141*, 626–634.

(4) (a) Troadec, T.; Wasano, T.; Lenk, R.; Baceiredo, A.; Saffon Merceron, N.; Hashizume, D.; Saito, Y.; Nakata, N.; Branchadell, V.; Kato, T. Donor Stabilized Silylene/Phosphine Supported Carbon(0) Center with High Electron Density. *Angew. Chem., Int. Ed.* **2017**, *56*, 6891–6895. (b) Wang, H.; Wu, L.; Lin, Z.; Xie, Z. Synthesis, Structure and Reactivity of a Borylene Cation [(NHSi)<sub>2</sub>B(CO)]<sup>+</sup> Stabilized by Three Neutral Ligands. *J. Am. Chem. Soc.* **2017**, *139*, 13680–13683. (c) Wang, Y.; Karni, M.; Yao, S.; Apeloig, Y.; Driess, M. An Isolable Bis(silylene) Stabilized Germylene and Its Reactivity. *J. Am. Chem. Soc.* **2019**, *141*, 1655–1664.

(5) Blom, B.; Gallego, D.; Driess, M. N Heterocyclic Silylene Complexes in Catalysis: New Frontiers in an Emerging Field. *Inorg. Chem. Front.* **2014**, *1*, 134–148.

(6) Zhou, Y. P.; Driess, M. Isolable Silylene Ligands Can Boost Efficiencies and Selectivities in Metal Mediated Catalysis. *Angew. Chem., Int. Ed.* **2019**, *58*, 3715–3728.

(7) Fürstner, A.; Krause, H.; Lehmann, C. W. Preparation, Structure and Catalytic Properties of a Binuclear Pd(0) Complex with Bridging Silylene Ligands. *Chem. Commun.* **2001**, 2372–2373.

(8) Zhang, M.; Liu, X.; Shi, C.; Ren, C.; Ding, Y.; Roesky, H. W. The Synthesis of ( $\eta^3$ -C<sub>3</sub>H<sub>5</sub>)Pd{Si[N(<sup>t</sup>Bu)CH]<sub>2</sub>}Cl and the Catalytic Property for Heck Reaction. *Z. Anorg. Allg. Chem.* **2008**, *634*, 1755–1758.

(9) Someya, C. I.; Haberberger, M.; Wang, W.; Enthaler, S.; Inoue, S. Application of a Bis(silylene) Nickel Complex as Precatalyst in C–C Bond Formation Reactions. *Chem. Lett.* **2013**, *42*, 286–288.

(10) Tan, G.; Enthaler, S.; Inoue, S.; Blom, B.; Driess, M. Synthesis of Mixed Silylene–Carbene Chelate Ligands from N Heterocyclic Silylcarbenes Mediated by Nickel. *Angew. Chem., Int. Ed.* **2015**, *54*, 2214–2218.

(11) Qi, X.; Sun, H.; Li, X.; Fuhr, O.; Fenske, D. Synthesis and Catalytic Activity of N Heterocyclic Silylene (NHSi) Cobalt Hydride for Kumada Coupling Reactions. *Dalton Trans* **2018**, *47*, 2581–2588.

(12) Gallego, D.; Brück, A.; Irran, E.; Meier, F.; Kaupp, M.; Driess, M.; Hartwig, J. F. From Bis(silylene) and Bis(germylene) Pincer Type Nickel(II) Complexes to Isolable Intermediates of the Nickel Catalyzed Sonogashira Cross Coupling Reaction. *J. Am. Chem. Soc.* **2013**, *135*, 15617–15626.

(13) Brück, A.; Gallego, D.; Wang, W.; Irran, E.; Driess, M.; Hartwig, J. F. Pushing the  $\sigma$  Donor Strength in Iridium Pincer Complexes: Bis(silylene) and Bis(germylene) Ligands Are Stronger Donors than Bis(phosphorus(III)) Ligands. *Angew. Chem., Int. Ed.* **2012**, *51*, 11478–11482.

(14) Ren, H.; Zhou, Y. P.; Bai, Y.; Cui, C.; Driess, M. Cobalt Catalyzed Regioselective Borylation of Arenes: N Heterocyclic Silylene as an Electron Donor in the Metal Mediated Activation of C–H Bonds. *Chem. Eur. J.* **2017**, *23*, 5663–5667.

(15) Wang, W.; Inoue, S.; Enthaler, S.; Driess, M. Bis(silylenyl) and Bis(germylenyl) Substituted Ferrocenes: Synthesis, Structure, and Catalytic Applications of Bidentate Silicon(II)–Cobalt Complexes. *Angew. Chem., Int. Ed.* **2012**, *51*, 6167–6171.

(16) Blom, B.; Enthaler, S.; Inoue, S.; Irran, E.; Driess, M. Electron Rich N Heterocyclic Silylene (NHSi) – Iron Complexes: Synthesis, Structures, and Catalytic Ability of an Isolable Hydridosilylene–Iron Complex. *J. Am. Chem. Soc.* **2013**, *135*, 6703–6713.

(17) Gallego, D.; Inoue, S.; Blom, B.; Driess, M. Highly Electron Rich Pincer Type Iron Complexes Bearing Innocent Bis(metallylene) pyridine Ligands: Syntheses, Structures, and Catalytic Activity. *Organometallics* **2014**, *33*, 6885–6897.

(18) Metsänen, T. T.; Gallego, D.; Szilvási, T.; Driess, M.; Oestreich, M. Peripheral Mechanism of a Carbonyl Hydrosilylation Catalysed by an SiNSi Iron Pincer Complex. *Chem. Sci.* **2015**, *6*, 7143–7149.

(19) Iimura, T.; Akasaka, N.; Iwamoto, T. A Dialkylsilylene Pt(0) Complex with a DVTMS Ligand for the Catalytic Hydrosilylation of Functional Olefins. *Organometallics* **2016**, *35*, 4071–4076.

(20) Iimura, T.; Akasaka, N.; Kosai, T.; Iwamoto, T. A Pt(0) Complex with Cyclic (alkyl)(amino)silylene and 1,3-Divinyl 1,1,3,3-



tetramethyldisiloxane Ligands: Synthesis, Molecular Structure, and Catalytic Hydrosilylation Activity. *Dalton Trans* **2017**, *46*, 8868–8874.

(21) Wang, Y.; Kostenko, A.; Yao, S.; Driess, M. Divalent Silicon Assisted Activation of Dihydrogen in a Bis(N heterocyclic silylene) xanthene Nickel(0) Complex for Efficient Catalytic Hydrogenation of Olefins. *J. Am. Chem. Soc.* **2017**, *139*, 13499–13506.

(22) Luecke, M. P.; Porwal, D.; Kosrenko, A.; Zhou, Y. P.; Yao, S.; Keck, M.; Limberg, C.; Oestreich, M.; Driess, M. Bis(silylenyl) substituted ferrocene stabilized  $\eta^6$  arene iron(0) complexes: synthesis, structure and catalytic application. *Dalton Trans* **2017**, *46*, 16412–16418.

(23) Zhou, Y. P.; Mo, Z.; Luecke, M. P.; Driess, M. Stereoselective Transfer Semi Hydrogenation of Alkynes to E Olefins with N Heterocyclic Silylene–Manganese Catalysts. *Chem. Eur. J.* **2018**, *24*, 4780–4784.

(24) Wang, W.; Inoue, S.; Irran, E.; Driess, M. Synthesis and Unexpected Coordination of a Silicon(II) Based SiCSi Pincerlike Arene to Palladium. *Angew. Chem., Int. Ed.* **2012**, *51*, 3691–3694.

(25) (a) Gelman, D.; Musa, S. Coordination Versatility of  $sp^3$  Hybridized Pincer Ligands toward Ligand–Metal Cooperative Catalysis. *ACS Catal.* **2012**, *2*, 2456–2466. (b) Wendt, O. F. Transition Metal Pincer Complexes with a Central  $sp^3$  Hybridized Carbon Atom. In *Pincer Compounds*; Elsevier: 2018; pp 237–250.

(26) (a) Tanabe, Y.; Nishibayashi, Y. Developing More Sustainable Processes for Ammonia Synthesis. *Coord. Chem. Rev.* **2013**, *257*, 2551–2564. (b) Van der Ham, C. J. M.; Koper, M. T. M.; Hetterscheid, D. G. H. Challenges in Reduction of Dinitrogen by Proton and Electron Transfer. *Chem. Soc. Rev.* **2014**, *43*, 5183–5191. (c) Köthe, C.; Limberg, C. Late Metal Scaffolds that Activate Both, Dinitrogen and Reduced Dinitrogen Species  $N_xH_y$ . *Z. Anorg. Allg. Chem.* **2015**, *641*, 18–30. (d) Nishibayashi, Y. Recent Progress in Transition Metal Catalyzed Reduction of Molecular Dinitrogen under Ambient Reaction Conditions. *Inorg. Chem.* **2015**, *54*, 9234–9247. (e) Tanabe, Y.; Nishibayashi, Y. Catalytic Dinitrogen Fixation to Form Ammonia at Ambient Reaction Conditions Using Transition Metal Dinitrogen Complexes. *Chem. Rec.* **2016**, *16*, 1549–1577. (f) Burford, R. J.; Fryzuk, M. D. Examining the Relationship between Coordination Mode and Reactivity of Dinitrogen. *Nat. Rev. Chem.* **2017**, *1*, 0026.

(27) Yandulov, D. V.; Schrock, R. R. Catalytic Reduction of Dinitrogen to Ammonia at a Single Molybdenum Center. *Science* **2003**, *301*, 76–78.

(28) (a) Schrock, R. R. Catalytic Reduction of Dinitrogen to Ammonia by Molybdenum: Theory versus Experiment. *Angew. Chem., Int. Ed.* **2008**, *47*, 5512–5522. (b) Arashiba, K.; Miyake, Y.; Nishibayashi, Y. A Molybdenum Complex Bearing PNP type Pincer Ligands Leads to the Catalytic Reduction of Dinitrogen into Ammonia. *Nat. Chem.* **2011**, *3*, 120–125. (c) Kinoshita, E.; Arashiba, K.; Kuriyama, S.; Miyake, Y.; Shimazaki, R.; Nakanishi, H.; Nishibayashi, Y. Synthesis and Catalytic Activity of Molybdenum–Dinitrogen Complexes Bearing Unsymmetric PNP Type Pincer Ligands. *Organometallics* **2012**, *31*, 8437–8443. (d) Tanaka, H.; Arashiba, K.; Kuriyama, S.; Sasada, A.; Nakajima, K.; Yoshizawa, K.; Nishibayashi, Y. Unique Behaviour of Dinitrogen Bridged Dimolybdenum Complexes Bearing Pincer Ligand towards Catalytic Formation of Ammonia. *Nat. Commun.* **2014**, *5*, 3737. (e) Kuriyama, S.; Arashiba, K.; Nakajima, K.; Tanaka, H.; Kamaru, N.; Yoshizawa, K.; Nishibayashi, Y. Catalytic Formation of Ammonia from Molecular Dinitrogen by Use of Dinitrogen Bridged Dimolybdenum–Dinitrogen Complexes Bearing PNP Pincer Ligands: Remarkable Effect of Substituent at PNP Pincer Ligand. *J. Am. Chem. Soc.* **2014**, *136*, 9719–9731. (f) Arashiba, K.; Kinoshita, E.; Kuriyama, S.; Eizawa, A.; Nakajima, K.; Tanaka, H.; Yoshizawa, K.; Nishibayashi, Y. Catalytic Reduction of Dinitrogen to Ammonia by Use of Molybdenum Nitride Complexes Bearing a Tridentate Triphosphine as Catalysts. *J. Am. Chem. Soc.* **2015**, *137*, 5666–5669. (g) Arashiba, K.; Eizawa, A.; Tanaka, H.; Nakajima, K.; Yoshizawa, Y.; Nishibayashi, Y. Catalytic Nitrogen Fixation via Direct Cleavage of Nitrogen–Nitrogen Triple

Bond of Molecular Dinitrogen under Ambient Reaction Conditions. *Bull. Chem. Soc. Jpn.* **2017**, *90*, 1111–1118. (h) Eizawa, A.; Arashiba, K.; Tanaka, H.; Kuriyama, S.; Matsuo, Y.; Nakajima, K.; Yoshizawa, K.; Nishibayashi, Y. Remarkable Catalytic Activity of Dinitrogen Bridged Dimolybdenum Complexes Bearing NHC based PCP Pincer Ligands toward Nitrogen Fixation. *Nat. Commun.* **2017**, *8*, 14874.

(29) Lukoyanov, D.; Khadka, N.; Yang, Z. Y.; Dean, D. R.; Seefeldt, L. C.; Hoffman, B. M. Reductive Elimination of  $H_2$  Activates Nitrogenase to Reduce the  $N\equiv N$  Triple Bond: Characterization of the  $E_4(4H)$  Janus Intermediate in Wild Type Enzyme. *J. Am. Chem. Soc.* **2016**, *138*, 10674–10683.

(30) Kandemir, T.; Schuster, M. E.; Senyshyn, A.; Behrens, M.; Schlögl, R. The Haber–Bosch Process Revisited: On the Real Structure and Stability of “Ammonia Iron” under Working Conditions. *Angew. Chem., Int. Ed.* **2013**, *52*, 12723–12726.

(31) (a) Anderson, J. S.; Rittle, J.; Peters, J. C. Catalytic Conversion of Nitrogen to Ammonia by an Iron Model Complex. *Nature* **2013**, *501*, 84–88. (b) Creutz, S. E.; Peters, J. C. Catalytic Reduction of  $N_2$  to  $NH_3$  by an Fe– $N_2$  Complex Featuring a C Atom Anchor. *J. Am. Chem. Soc.* **2014**, *136*, 1105–1115. (c) Del Castillo, T. J.; Thompson, N. B.; Suess, D. L. M.; Ung, G.; Peters, J. C. Evaluating Molecular Cobalt Complexes for the Conversion of  $N_2$  to  $NH_3$ . *Inorg. Chem.* **2015**, *54*, 9256–9262.

(32) (a) Kuriyama, S.; Arashiba, K.; Nakajima, K.; Matsuo, Y.; Tanaka, H.; Ishii, K.; Yoshizawa, K.; Nishibayashi, Y. Catalytic Transformation of Dinitrogen into Ammonia and Hydrazine by Iron Dinitrogen Complexes Bearing Pincer Ligand. *Nat. Commun.* **2016**, *7*, 12181. (b) Sekiguchi, Y.; Kuriyama, S.; Eizawa, A.; Arashiba, K.; Nakajima, K.; Nishibayashi, Y. Synthesis and Reactivity of Iron–Dinitrogen Complexes Bearing Anionic Methyl and Phenyl Substituted Pyrrole based PNP Type Pincer Ligands toward Catalytic Nitrogen Fixation. *Chem. Commun.* **2017**, *53*, 12040–12043.

(33) Hill, P. J.; Doyle, L. R.; Crawford, A. D.; Myers, W. K.; Ashley, A. E. Selective Catalytic Reduction of  $N_2$  to  $N_2H_4$  by a Simple Fe Complex. *J. Am. Chem. Soc.* **2016**, *138*, 13521–13524.

(34) (a) Tanabe, Y.; Nishibayashi, Y. Recent advances in catalytic silylation of dinitrogen using transition metal complexes. *Coord. Chem. Rev.* **2019**, *389*, 73–93. (b) Yin, J.; Li, J.; Wang, G. X.; Yin, Z. B.; Zhang, W. X.; Xi, Z. Dinitrogen Functionalization Affording Chromium Hydrazido Complex. *J. Am. Chem. Soc.* **2019**, *141*, 4241–4247.

(35) Yuki, M.; Tanaka, H.; Sasaki, K.; Miyake, Y.; Yoshizawa, K.; Nishibayashi, Y. Iron Catalysed Transformation of Molecular Dinitrogen into Silylamine under Ambient Conditions. *Nat. Commun.* **2012**, *3*, 1254.

(36) Ung, G.; Peters, J. C. Low Temperature  $N_2$  Binding to Two Coordinate  $L_2Fe^0$  Enables Reductive Trapping of  $L_2FeN_2^-$  and  $NH_3$  Generation. *Angew. Chem., Int. Ed.* **2015**, *54*, 532–535.

(37) Prokopchuk, D. E.; Wiedner, E. S.; Walter, E. D.; Popescu, C. V.; Piro, N. A.; Scott Kassel, W.; Morris Bullock, R.; Mock, M. T. Catalytic  $N_2$  Reduction to Silylamines and Thermodynamics of  $N_2$  Binding at Square Planar Fe. *J. Am. Chem. Soc.* **2017**, *139*, 9291–9301.

(38) Imayoshi, R.; Nakajima, K.; Takaya, J.; Iwasawa, N.; Nishibayashi, Y. Synthesis and Reactivity of Iron– and Cobalt–Dinitrogen Complexes Bearing PSiP Type Pincer Ligands toward Nitrogen Fixation. *Eur. J. Inorg. Chem.* **2017**, *2017*, 3769–3778.

(39) (a) Ferreira, R. B.; Cook, B. J.; Knight, B. J.; Catalano, V. J.; García Serres, R.; Murray, L. J. Catalytic Silylation of Dinitrogen by a Family of Triiron Complexes. *ACS Catal.* **2018**, *8*, 7208–7212. (b) Piascik, A. D.; Li, R.; Wilkinson, H. J.; Green, J. C.; Ashley, A. E. Fe Catalyzed Conversion of  $N_2$  to  $N(SiMe_3)_3$  via an Fe Hydrazido Resting State. *J. Am. Chem. Soc.* **2018**, *140*, 10691–10694.

(40) Bai, Y.; Zhang, J.; Cui, C. An Arene Tethered Silylene Ligand Enabling Reversible Dinitrogen Binding to Iron and Catalytic Silylation. *Chem. Commun.* **2018**, *54*, 8124–8127.

(41) (a) Schmedake, T. A.; Haaf, M.; Apeloig, Y.; Müller, T.; Bukalov, S.; West, R. Reversible Transformation between a Diaminosilylene and a Novel Disilene. *J. Am. Chem. Soc.* **1999**, *121*,

- 9479–9480. (b) Ichinohe, M.; Kinjo, R.; Sekiguchi, A. The First Stable Methyl Substituted Disilene: Synthesis, Crystal Structure, and Regiospecific MeLi Addition. *Organometallics* **2003**, *22*, 4621–4623.
- (c) Sasamori, T.; Hironaka, K.; Sugiyama, Y.; Takagi, N.; Nagase, S.; Hosoi, Y.; Furukawa, Y.; Tokitoh, N. Synthesis and Reactions of a Stable 1,2 Diaryl 1,2 dibromodisilene: A Precursor for Substituted Disilenes and a 1,2 Diaryldisilyne. *J. Am. Chem. Soc.* **2008**, *130*, 13856–13857. (d) Zhang, S. H.; Yeong, H. X.; Xi, H. W.; Lim, K. H.; So, C. W. Hydrosilylation of a Silicon(II) Hydride: Synthesis and Characterization of a Remarkable Silylsilylene. *Chem. Eur. J.* **2010**, *16*, 10250–10254. (e) Zhang, S. H.; Yeong, H. X.; So, C. W. Reactivity of a Silylsilylene Bearing a Functionalized Diaminochlorosilyl Substituent. *Chem. Eur. J.* **2011**, *17*, 3490–3499.
- (42) Zhu, G.; Li, X.; Xu, G.; Wang, L.; Sun, H. A New PC(sp<sup>3</sup>)P Ligand and Its Coordination Chemistry with Low Valent Iron, Cobalt and Nickel Complexes. *Dalton Trans* **2014**, *43*, 8595–8598.
- (43) Qi, X.; Zheng, T.; Zhou, J.; Dong, Y.; Zuo, X.; Li, X.; Sun, H.; Fuhr, O.; Fenske, D. Synthesis and Catalytic Activity of Iron Hydride Ligated with Bidentate N Heterocyclic Silylenes for Hydroboration of Carbonyl Compounds. *Organometallics* **2019**, *38*, 268–277.
- (44) (a) Schmedake, T. A.; Haaf, M.; Paradise, B. J.; Millevolte, A. J.; Powell, D. R.; West, R. Electronic and Steric Properties of Stable Silylene Ligands in Metal(0) Carbonyl Complexes. *J. Organomet. Chem.* **2001**, *636*, 17–25. (b) Yang, W.; Fu, H.; Wang, H.; Chen, M.; Ding, Y.; Roesky, H. W.; Jana, A. A Base Stabilized Silylene with a Tricoordinate Silicon Atom as a Ligand for a Metal Complex. *Inorg. Chem.* **2009**, *48*, 5058–5060.
- (45) Tobita, H.; Matsuda, A.; Hashimoto, H.; Ueno, K.; Ogino, H. Direct Evidence for Extremely Facile 1,2 and 1,3 Group Migrations in an FeSi<sub>2</sub> System. *Angew. Chem., Int. Ed.* **2004**, *43*, 221–224.
- (46) Sen, S. S.; Roesky, H. W.; Stern, D.; Henn, J.; Stalke, D. High Yield Access to Silylene RSiCl (R = PhC(NtBu)<sub>2</sub>) and Its Reactivity toward Alkyne: Synthesis of Stable Disilacyclobutene. *J. Am. Chem. Soc.* **2010**, *132*, 1123–1126.
- (47) Karsch, H. H. Funktionelle Trimethylphosphinderivate, V. Kovalente Methyleisen (II) Phosphinkomplexe. *Chem. Ber.* **1977**, *110*, 2699–2711.
- (48) Weitz, I. S.; Rabinovitz, M. The Application of C<sub>8</sub>K for Organic Synthesis: Reduction of Substituted Naphthalenes. *J. Chem. Soc., Perkin Trans. 1* **1993**, *1*, 117–120.
- (49) Palatinus, L.; Chapuis, G. SUPERFLIP. A Computer Program for the Solution of Crystal Structures by Charge Flipping in Arbitrary Dimensions. *J. Appl. Crystallogr.* **2007**, *40*, 786–790.
- (50) Sheldrick, G. M. A Short History of SHELX. *Acta Crystallogr., Sect. A: Found. Crystallogr.* **2008**, *A64*, 112–122.
- (51) Dolomanov, O. V.; Bourhis, L. J.; Gildea, R. J.; Howard, J. A. K.; Puschmann, H. OLEX2: A Complete Structure Solution, Refinement and Analysis Program. *J. Appl. Crystallogr.* **2009**, *42*, 339–341.